Dalton Transactions

Accepted Manuscript

This article can be cited before page numbers have been issued, to do this please use: K. S. Min, J. W. Shin, A. R. Jeong, S. Y. Lee, C. Kim and S. Hayami, *Dalton Trans.*, 2016, DOI: 10.1039/C6DT02701F.

ROYAL SOCIETY OF CHEMISTRY

www.rsc.org/dalton

View Article Online
DOI: 10.1039/C6DT02701F

Trinuclear nickel and cobalt complexes containing unsymmetrical tripodal tetradentate ligands: syntheses, structural, magnetic, and catalytic properties

Jong Won Shin,[a] Ah Rim Jeong,[a] Sun Young Lee,[b] Cheal Kim,*[,b] Shinya Hayami,[c] and Kil Sik Min*[,d]

[a] Department of Chemistry, Kyungpook National University, Daegu 41566, Republic of Korea

[b] Department of Fine Chemistry, Seoul National University of Science and Technology, Seoul 01811, Republic of Korea

[c] Department of Chemistry, Graduate School of Science and Technology, Kumamoto University, Kumamoto 860-8555, Japan

[d] Department of Chemistry Education, Kyungpook National University, Daegu 41566, Republic of Korea

E-mail: minks@knu.ac.kr (K. S. M.), chealkim@seoultech.ac.kr (C. K.)

View Article Online
DOI: 10.1039/C6DT02701F

Abstract

The coordination chemistries of the tetradentate N_2O_2-type ligands *N*-(2-pyridylmethyl)iminodiethanol (H_2pmide) and *N*-(2-pyridylmethyl)iminodiisopropanol (H_2pmidip) have been investigated with nickel(II) and cobalt(II/III) ions. Three novel complexes prepared and characterized are $[(Hpmide)_2Ni_3(CH_3COO)_4]$ (**1**), $[(Hpmide)_2Co_3(CH_3COO)_4]$ (**2**), and $[(pmidip)_2Co_3(CH_3COO)_4]$ (**3**). In **1** and **2**, two terminal nickel(II)/cobalt(II) units are coordinated to one $Hpmide^-$ and two $CH_3CO_2^-$. The terminal units are each connected to a central nickel(II)/cobalt(II) cation through one oxygen atom of $Hpmide^-$ and two oxygen atoms of acetate ions, giving rise to nickel(II) and cobalt(II) trinuclear complexes, respectively. Trinuclear complexes **1** and **2** are isomorphous. In **3**, two terminal cobalt(III) units are coordinated to $pmidip^{2-}$ and two $CH_3CO_2^-$. The terminal units are each linked to a central cobalt(II) cation through two oxygen atoms of $pmidip^{2-}$ and one oxygen atom of a bidentate acetate ion, resulting to a linear trinuclear mixed-valence cobalt complex. **1** shows a weak ferromagnetic interaction through the ethoxo and acetato groups between the nickel(II) ions (g = 2.24, J = 2.35 cm^{-1}). However, **2** indicates a weak antiferromagnetic coupling through the ethoxo and acetato groups between the cobalt(II) ions (g = 2.37, J = –0.5 cm^{-1}). Additionally, **3** behaves as a paramagnetic cobalt(II) monomer, due to the diamagnetic cobalt(III) ions in the terminal units (g = 2.53, $|D|$ = 36.0 cm^{-1}). No catalytic activity was observed in **1**. However, **2** and **3** showed significant catalytic activities toward various olefins with modest to good yields. **3** was slightly less efficient toward olefin epoxidation reaction than **2**. Also **2** was used for terminal olefin oxidation reaction and showed the oxidation to the corresponding epoxides in moderate yields (34-75%) with conversions (47-100%). The cobalt complexes **2** and **3** promoted the O-O bond cleavage to ~75% heterolysis and ~25% homolysis.

View Article Online
DOI: 10.1039/C6DT02701F

Introduction

Multinuclear coordination compounds incorporating polynucleating ligands have received considerable interest, because of their interesting structures and potential applications in molecular magnetism and catalysis.[1–3] The introduction of hydroxyl group in polynucleating ligands is able to form a variety of multinuclear and polymeric compounds, due to deprotonation of the group.[4] In this context, tetradentate tripodal ligands including hydroxyl group have been used for preparation of various multinuclear transition metal complexes.[5] The deprotonation of the hydroxyl-based tetradentate ligands forms hydroxo-bridged multinuclear coordination compounds.

In previous studies we have reported tri-/tetranuclear complexes based on an N_3O-type *N*,*N*–bis(2-pyridylmethyl)-2-aminoethanol (bpaeOH) ligand. The complexes are a mixed-valence trinuclear cobalt complex $[Co_3(bpaeO)_2(NO_3)(N_3)_4](NO_3)$ and a tetranuclear iron(III) complex $[Fe_4(bpaeO)_2(CH_3O)_2(N_3)_8]$. The former is a paramagnetic species as Co(III)-Co(II)-Co(III) trimer and shows efficient catalytic activities in the olefin epoxidation and alcohol oxidation reactions, and the latter displays interesting magnetic properties with both ferro- and antiferromagnetic interactions between the iron(III) ions.[6]

Furthermore, the use of N_2O_2-type ligand *N*-(2-pyridylmethyl)iminodiethanol (H_2pmide) induces more diverse structures in coordination compounds, due to the deprotonation of two hydroxyl groups. Until now, six multinuclear coordination compounds based on *N*-(2-pyridylmethyl)iminodiethanol (H_2pmide) have been reported and studied. First, dinuclear complexes, $[(Hpmide)Fe(NO_3)]_2(NO_3)_2{\bullet}2CH_3OH$, $[(pmide)Fe(N_3)]_2$, and $[Cu(H_2pmide)(NO_3)Cu(Hpmide)](NO_3)_2$ have been prepared and characterized.[7,8] The iron(III) dinuclear complexes have mono- and di-deprotonated H_2pmide ligands depending on anions and show different magnetic interactions and catalytic effects depending on the different conformations.[7] In the case of the copper(II) dimer, it has an asymmetric structure and exhibits a strong antiferromagnetic coupling.[8] Second, trinuclear complexes $[\{Ni(Hpmide)\}_2Ni(CH_3CO_2)_2(HCO_2)_2]$ and $[(pmide)_2Co_3(CH_3CO_2)_2(NCS)_2]{\cdot}4CH_3OH$ have been reported. In the nickel(II) trimer, the Ni(Hpmide) units are each connected to a central nickel(II) cation through the μ_2-oxygen of $Hpmide^-$, one μ_1-bridged acetate, and one μ_2-bridged formate.[9] Unfortunately, the magnetic data of the nickel(II) trimer have not been reported. The latter is composed of two terminal subunits $\{Co(pmide)(NCS)(CH_3CO_2)\}^-$ and a central cobalt(II) cation. The terminal units are each linked to a central cobalt(II) cation via two μ_2-oxygen of $pmide^{2-}$ and one μ_2-

View Article Online
DOI: 10.1039/C6DT02701F

bridged acetate.[8] This is a mixed-valence Co(III)-Co(II)-Co(III) trimeric complex and shows a paramagnetic property with large ZFS value. Third, octanuclear complex $[Mn_8O_4(Hpmide)_4(EtCO_2)_6]\bullet(ClO_4)_2$ has been reported. The structure of the octamer shows four manganese(II) and four manganese(III) ions and has three face-sharing cubes with manganese cations on alternate corners. The octamer behaves as a single-molecule-magnet and also displays a spin-frustration effect.[10]

In the efforts to explore the role of metal ions, anions and ligands, we have synthesized three trinuclear coordination compounds based on H_2pmide and H_2pmidip ligands (H_2pmide = *N*-(2-pyridylmethyl)iminodiethanol, H_2pmidip = *N*-(2-pyridylmethyl)iminodiisopropanol). That is, the trinuclear complexes can be shown significant structures, magnetic and catalytic properties by controlling the factors, i.e., metal ion, anion, and ligand. The H_2pmidip ligand is prepared and characterized as a new ligand to check electronic and steric effects for multinuclear coordination compounds. Herein, we report the synthesis, crystal structure, magnetic properties, and catalytic activity of bis-ethoxy-bridged trinickel(II) complex $[(Hpmide)_2Ni_3(CH_3COO)_4]$ (**1**), tricobalt(II) complex $[(Hpmide)_2Co_3(CH_3COO)_4]$ (**2**), and mixed-valence cobalt trinuclear complex $[(pmidip)_2Co_3(CH_3COO)_4]$ (**3**). Interestingly, complexes **1** and **2** are shown antiferromagnetic and ferromagnetic interactions, respectively. In contrast to **1**, complexes **2** and **3** exhibited significant catalytic activities toward a variety of olefins.

Experimental

General

All chemicals used in the synthesis were of reagent grade and used without further purification. *N*-(2-Pyridylmethyl)iminodiethanol (H_2pmide) was prepared according to the literature procedure.[10] Olefins, epoxides, 2-cyclohexen-1-ol, 2-cyclohexen-1-one, benzaldehyde, acetonitrile, dichloromethane, dodecane, MCPBA (65%) were purchased from Aldrich Chemical Co. and were used without further purification. PPAA was synthesized on reference to the method described in the literature.[11] UV/Vis absorption spectra were recorded with a SCINCO S-2100 spectrophotometer and a Perkin Elmer model Lambda 2S UV/Vis spectrometer. Infrared spectra were recorded with a Thermo Fisher Scientific IR200 spectrophotometer (±1 cm^{-1}) using KBr disk. Elemental analyses were carried out using a Fisons/Carlo Erba EA1108 instrument in air. ^{1}H-NMR spectra were measured on Bruker

View Article Online
DOI: 10.1039/C6DT02701F

AVANCE digital 400 spectrometer. X-ray powder diffraction (XRPD) patterns were measured at room temperature with the 120 mm detector distance in the 2θ range 5-50° on an ADSC Quantum-210 detector using synchrotron radiation (λ = 0.90013 Å, Si(111) double crystal monochromator) in the beamline 2D SMC at the Pohang Accelerator Laboratory (PAL), Korea. Magnetic susceptibilities were measured in applied field of 5000~10000 Oe between 2 and 300 K on a Quantum Design MPMS superconducting quantum interference device (SQUID) magnetometer. Diamagnetic corrections were made [404.1 (**1**), 411.1 (**2**), and 448.6 $\times$ 10^{-6} (**3**) emu/mol] by using Pascal's constants. Product analysis for olefin epoxidation and PPAA experiment was conducted by using Perkin Elmer gas chromatograph equipped with a FID detector and a 30 m capillary column (Hewlett-Packard, DB-5 or HP-FFAP).

Syntheses of compounds

***N*-(2-Pyridylmethyl)iminodiisopropanol (H_2pmidip).** Diisopropanolamine (6.50 g, 48.8 mmol) was dissolved in 60 mL isopropanol followed by the addition of 2-(chloromethyl)pyridine hydrochloride (8.0 g, 48.8 mmol) and sodium carbonate (5.13 g, 48.8 mmol), then was refluxed overnight. The resultant solution was evaporated to dryness and 100 mL dichloromethane was added and a white precipitate was filtered. The dichloromethane solution was washed by concentrated brine and dried by $MgSO_4$. After removing the organic solvent, pale red oil was obtained and used without further purification. Yield: 5.93 g (54%). ^{1}H NMR (400 MHz, D_2O, 297 K): δ = 0.96 (dd, J = 4, 4 Hz, 6H), 2.30~2.52 (m, 4H), 3.54~3.83 (m, 4H), 7.24 (t, J = 4 Hz, 1H), 7.37 (d, J = 4 Hz, 1H), 7.71 (t, J = 8 Hz, 1H), 8.33 (d, J = 4 Hz, 1H).

[(Hpmide)$_2$Ni$_3$(CH$_3$COO)$_4$] (1). To a methanol solution (2 mL) of Ni(CH$_3$COO)$_2$•4H$_2$O (149 mg, 0.60 mmol) was added dropwise an acetonitrile solution (4 mL) of H_2pmide (79 mg, 0.40 mmol), and the solution was stirred for 30 min at room temperature. Green crystals of **1** were obtained by diffusion of diethyl ether into the green solution for several days, and were collected by filtration and washed with diethyl ether and dried in air. Yield: 63 mg (39%). FT-IR (KBr, cm^{-1}): 3422, 3089, 2927, 2871, 1582, 1540, 1417. Anal Calcd for $C_{28}H_{43}N_4Ni_3O_{12.5}$: C, 41.43; H, 5.34; N, 6.90. Found: C, 41.47; H, 5.40; N, 6.72.

[(Hpmide)$_2$Co$_3$(CH$_3$COO)$_4$] (2). To a methanol solution (2 mL) of Co(CH$_3$COO)$_2$•4H$_2$O (150 mg, 0.60 mmol) was added dropwise an acetonitrile solution (4 mL) of H_2pmide (79 mg, 0.40 mmol), and

View Article Online
DOI: 10.1039/C6DT02701F

the color became purple, and the solution was stirred for 30 min at room temperature. Purple crystals of **2** were obtained by diffusion of diethyl ether into the purple solution for several days, and were collected by filtration and washed with diethyl ether and dried in air. Yield: 127 mg (79%). FT-IR (KBr, cm^{-1}): 3427, 3083, 2927, 2879, 1604, 1575, 1412, 1339, 1275, 1083, 920, 890, 772. Anal. Calcd for $C_{28}H_{42}Co_3N_4O_{12}$: C, 41.86; H, 5.27; N, 6.97. Found: C, 41.73; H, 5.39; N, 7.03.

[(pmidip)$_2$Co$_3$(CH$_3$COO)$_4$] (3). To a methanol solution (2 mL) of $Co(CH_3COO)_2 \cdot 4H_2O$ (75 mg, 0.30 mmol) was added dropwise an acetonitrile solution (4 mL) of H_2pmidip (45 mg, 0.20 mmol), and the color became purple, and the solution was stirred for 30 min at room temperature. Dark violet crystals of **3** were obtained by diffusion of diethyl ether into the purple solution for several days, and were collected by filtration and washed with diethyl ether and dried in air. Yield: 42 mg (49%). FT-IR (KBr, cm^{-1}): 3410, 3044, 2966, 2857, 1591, 1570, 1414, 1376, 1313, 1140, 1065, 945, 867, 692. Anal. Calcd for $C_{32}H_{50}Co_3N_4O_{13}$: C, 43.90; H, 5.76; N, 6.40. Found: C, 43.88; H, 5.68; N, 6.47.

Catalytic olefin epoxidations by MCPBA in the presence of cobalt complexes

MCPBA (0.07 mmol) was added to a mixture of substrate (0.035 mmol) and complex (**2** or **3**, 1.24 x 10^{-3} mmol) in CH_3CN/CH_2Cl_2 (1:1 v/v; 1 mL). The mixture was stirred for 10 min at room temperature. The reaction was monitored by GC/mass analysis of 20 μL aliquots withdrawn periodically from the reaction mixture. Dodecane as an internal standard was used to quantify the yields of products and conversions of substrates. All reactions were run at least three times, and the average conversions and product yields are presented. Conversions and product yields were based on substrate.

Analysis of the O−O bond cleavage products from the oxidation reactions of substrates by PPAA in the presence of cobalt complexes

PPAA (0.04 mmol) was added to a mixture of substrate (0–0.16 mmol) and complex (**2** or **3**, 1.24 x 10^{-3} mmol) in CH_3CN/CH_2Cl_2 (1:1 v/v; 1 mL). The mixture was stirred for 10 min at room temperature. The reaction was monitored by GC/mass analysis of 20 μL aliquots withdrawn periodically from the reaction mixture. Dodecane as an internal standard was used to quantify the yields of products and conversions of substrates. All reactions were run at least three times, and the average conversions and product yields are presented. Conversions and product yields were based on substrate or PPAA.

View Article Online
DOI: 10.1039/C6DT02701F

X-ray crystallographic data collection and refinement

Single crystals of **1** and **3** were coated with paratone-*N* oil and the diffraction data measured at 100(2)~102(2) K with synchrotron radiation (λ = 0.63000 Å) on an ADSC Quantum-210 detector at 2D SMC with a silicon (111) double crystal monochromator (DCM) at the Pohang Accelerator Laboratory, Korea. The ADSC Q210 ADX program[12] was used for data collection (detector distance is 63 mm, omega scan; $\Delta\omega$ = 1º, exposure time is 1 sec per frame) and HKL3000sm (Ver. 703r)[13] was used for cell refinement, reduction and absorption correction. Single crystals of **2** were mounted on a Bruker SMART APEX CCD-based diffractometer (Korea Basic Science Institute, Chonju Branch). X-ray data for **2** were collected at 200(2) K and using Mo Kα radiation (λ = 0.71073 Å, graphite monochromator). The raw data were processed to give structure factors using the Bruker SAINT program and corrected for Lorentz and polarization effects.[14] The crystal structures of **1**−**3** were solved by direct methods,[15] and refined by full-matrix least-squares refinement using the SHELXL-2013 computer program.[16] The positions of all non-hydrogen atoms were refined with anisotropic displacement factors. All hydrogen atoms were placed using a riding model, and their positions were constrained relative to their parent atoms using the appropriate HFIX command in SHELXL-2013, except the hydrogens of hydroxyl groups in **1**−**2**. The crystallographic data and the result of refinements are summarized in Table 1.

Chart 1

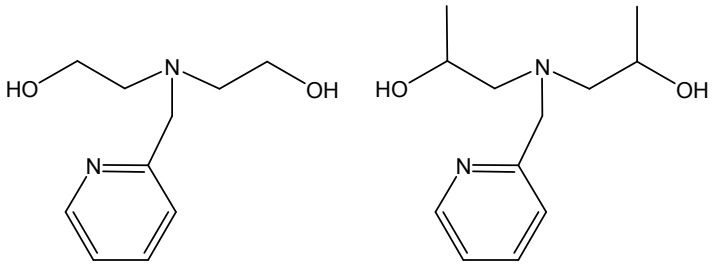

H_2pmide H_2pmidip

$[(Hpmide)_2Ni_3(CH_3COO)_4]$ (**1**)
$[(Hpmide)_2Co_3(CH_3COO)_4]$ (**2**)
$[(pmidip)_2Co_3(CH_3COO)_4]$ (**3**)

View Article Online
DOI: 10.1039/C6DT02701F

Results and discussion

Synthesis and characterization

The reaction of two equiv of H_2pmide and three equiv of $Ni(OAc)_2•4H_2O$ in methanol/acetonitrile under an aerobic condition affords air stable $[(Hpmide)_2Ni_3(CH_3COO)_4]$ (**1**) in moderate yield (39%). The complex is a linear trinuclear compound, which is formed through ethoxo and acetate groups. IR spectrum of **1** in KBr had peaks characteristic of coordinated $Hpmide^-$ and acetate anions. The IR spectrum of **1** showed strong absorptions at 1582 and 1417 cm^{-1} that are assigned to the acetate anions as bridging with nickel(II) ions.[17] The bands of the C−H of $Hpmide^-$ ligand appeared at 3089, 2927, and 2871 cm^{-1} and the band of the O−H of $Hpmide^-$ ligand appeared at 3422 cm^{-1}. The reaction of 2 equiv of H_2pmide and 3 equiv of $Co(OAc)_2•4H_2O$ in mixed solvent (MeOH/MeCN) under an aerobic condition affords air stable $[(Hpmide)_2Co_3(CH_3COO)_4]$ (**2**) in good yield (79%). As expected, the structure of **2** is the same to that of **1**. IR spectrum of **2** in KBr had peaks characteristic of coordinated $Hpmide^-$ and acetate anions. The IR spectrum of **2** showed strong absorptions at 1575 and 1412 cm^{-1} that are assigned to the acetate anions as bridging with cobalt(II) ions.[17] The bands of the C−H of $Hpmide^-$ ligand appeared at 3083, 2927, and 2879 cm^{-1} and the band of the O−H of $Hpmide^-$ ligand appeared at 3427 cm^{-1}. The reaction of 2 equiv of H_2pmidip and 3 equiv of $Co(OAc)_2•4H_2O$ in mixed solvent (MeOH/MeCN) under an aerobic condition affords air stable $[(pmidip)_2Co_3(CH_3COO)_4]$ (**3**) in moderate yield (49%). In this case, different to **2**, complex **3** is formed as a mixed-valence trimeric Co(III)−Co(II)−Co(III) species. This can be attributed to the basicity of the H_2pmidip ligand. IR spectrum of **3** in KBr had peaks characteristic of coordinated $pmidip^{2-}$ and acetate anions. The IR spectrum of **3** showed strong absorptions at 1570 and 1414 cm^{-1} that are assigned to the acetate anions as bridging with cobalt(II/III) ions.[17] The bands of the C−H of $pmidip^{2-}$ ligand appeared at 3044, 2966, and 2857 cm^{-1}. The composition of **1**−**3** was also identified by elemental analyses, infrared spectroscopy, and single crystal X-ray diffraction.

Description of crystal structures

Structure of 1. Compound **1** crystallizes in the monoclinic $P2_1/n$ space group, and the unit cell includes two trinuclear complexes, and the ORTEP drawing of **1** is shown in Fig. 1. The selected bond lengths and angles are listed in Table S1. The crystal structure of **1** consists of discrete centro-symmetric trinuclear unit of formula $[(Hpmide)_2Ni_3(CH_3COO)_4]$. The central nickel(II) ion (Ni2) which

View Article Online
DOI: 10.1039/C6DT02701F

lies on an inversion center is bonded to four oxygen atoms of acetate anions (av. Ni−$O_{acetate}$ = 2.091(1) Å) and to two bridged oxygen atoms of $Hpmide^-$ ligand (av. Ni−O_{Hpmide} = 2.024(1) Å). On the other hand, the terminal nickel(II) ions (Ni1) are bonded to two nitrogen atoms of $Hpmide^-$ ligand and two oxygen atoms from acetate anions (av. Ni−N_{Hpmide} = 2.093(1), Ni−$O_{acetato}$ = 2.077(1) Å) and to one bridged ethoxy group (Ni−O_{ethoxy} = 2.0036(9) Å) and to one oxygen atom of hydroxyl group in $Hpmide^-$ ligand (Ni−$O_{hydroxyl}$ = 2.1524(9) Å). All nickel ions adopt distorted octahedral geometries with two $Hpmide^-$ ligands and four acetate anions. The H_2pmide ligands in **1** are monodeprotonated to give $Hpmide^-$. The four acetate anions bind to the three nickel(II) ions in different modes. Two of them are $\mu_{1,3}$-acetato ligands for Ni1 and Ni2, and the other are $\mu_{1,1}$-acetato ligands for Ni1 and Ni2. The distorted octahedral coordination sphere of the central nickel (Ni2) involves an O_6 donor set including two μ-O_{alkoxo} ($Hpmide^-$), two O ($\mu_{1,3}$-acetato), and two O ($\mu_{1,1}$-acetato). The octahedral coordination sphere of the external nickel (Ni1) shows an N_2O_4 donor set including one N_{py} ($Hpmide^-$), N_{amine} ($Hpmide^-$), one O_{alkoxo} ($Hpmide^-$), $O_{hydroxyl}$ ($Hpmide^-$), one O ($\mu_{1,3}$-acetato), and one O ($\mu_{1,1}$-acetato). Two bridging Ni1−O1−Ni2 and Ni1−O6−Ni2 angles are 100.17(4) and 91.90(4)°, respectively. The Ni1•••Ni2 and Ni1•••Ni1(−x+1, −y, −z) distances within the trimeric cation are 3.0895(6) and 6.1790(12) Å, respectively.

Structure of 2. Compound **2** crystallizes in the monoclinic $P2_1/n$ space group, and the unit cell includes two trinuclear complexes, and the ORTEP drawing of **2** is shown in Fig. 2. The selected bond lengths and angles are listed in Table S2. The core structure of **2** is composed of one $Co^{II}Co^{II}Co^{II}$ trimer and four acetate anions. The central cobalt(II) ion (Co2) is bonded to four oxygen atoms of acetate anions (av. Co–$O_{acetate}$ = 2.153(2) Å) and to two bridged oxygen atoms of $Hpmide^-$ ligand (av. Co–O_{Hpmide} = 2.016(3) Å). On the other hand, the terminal cobalt(II) ions (Co1) are bonded to two nitrogen atoms of $Hpmide^-$ ligand and two oxygen atoms from acetate anions (av. Co–N_{Hmide} = 2.220(3), Co–$O_{acetate}$ = 2.055(3) Å) and to one bridged ethoxy group (Co–O_{ethoxy} = 1.987(4) Å), and to one oxygen atom of hydroxyl group in $Hpmide^-$ ligand (Co–$O_{hydroxyl}$ = 2.196(4) Å).[6b,18] All cobalt ions adopt distorted octahedral geometries with two $Hpmide^-$ ligands and four acetate anions. The H_2pmide ligands in **2** are monodeprotonated to give $Hpmide^-$. The four acetate anions bind to the three cobalt ions in different modes. Two of them are $\mu_{1,3}$-acetato ligands for Co1 and Co2, and the other are $\mu_{1,1}$-acetato ligands for Co1 and Co2. The distorted octahedral coordination sphere of the

View Article Online
DOI: 10.1039/C6DT02701F

central cobalt (Co2) involves an O_6 donor set including two μ-O_{alkoxo} ($Hpmide^-$), and two O ($\mu_{1,3}$-acetato), and two μ_2-O ($\mu_{1,1}$-acetato). The octahedral coordination sphere of the external cobalt (Co1) shows an N_2O_4 donor set including one N_{py} ($Hpmide^-$), N_{amine} ($Hpmide^-$), one O_{alkoxo} ($Hpmide^-$), $O_{hydroxyl}$ ($Hpmide^-$), one O ($\mu_{1,3}$-acetato), and one O ($\mu_{1,1}$-acetato). Two bridging Co1−O1−Co2 and Co1−O6−Co2 angles are 102.92(17) and 89.56(14)°, respectively. The Co1•••Co2 distance within the trimeric cation is 3.1314(2) Å and the bond distance compares well with those previously reported for cobalt(II) ions.[19] The Co1•••Co1 (-x+2, -y+1, -z) distance is 6.62627(4) Å and the shortest Co•••Co distance between the trimers is 7.2362(5) Å. The bond angles relating to the external cobalt (Co1) and internal cobalt (Co2) lie from 78.74(17) to 175.14(16)° and 80.14(15) to 180.00(16)°, respectively. According to the bond angles, the central cobalt (Co2) is closer to octahedral geometry than the external cobalt (Co1). The structure of **2** is isomorphous to that of **1**.

Structure of 3. Compound **3** crystallizes in the monoclinic $P2_1/c$ space group, and the unit cell includes two trinuclear complexes, and the ORTEP drawing of **3** is shown in Fig. 3. The selected bond lengths and angles are listed in Table S3. The core structure of **3** is composed of one mixed-valence $Co^{III}Co^{II}Co^{III}$ trimer bridged with oxygen atoms of $pmidip^{2-}$ and acetate ions. The central cobalt(II) ion is bonded to two oxygen atoms of acetate anions (av. Co2–$O_{acetate}$ = 2.098(2) Å) and to four oxygen atoms of $pmidip^{2-}$ ligand (av. Co2–O_{pmidip} = 2.117(1) Å). On the other hand, the terminal cobalt(III) ions are bonded to two nitrogen atoms of $pmidip^{2-}$ ligand and two oxygen atoms from acetate anions (av. Co1–N_{pmidip} = 1.941(1), Co1–$O_{acetate}$ = 1.927(1) Å) and to two bridged methyl ethoxy group (Co1–O = 1.895(1) Å).[6b,18,20] The bond distances relating to Co1 ion are in good agreement with those of low-spin cobalt(III) ions reported previously,[6b] while the bond lengths around Co2 ion are somewhat longer than those of Co2 ion and indicate a high-spin cobalt(II) ion.[21]

All cobalt ions adopt distorted octahedral geometries with two $pmidip^{2-}$ ligands and four acetate anions. The H_2pmidip ligands in **3** are fully deprotonated to give $pmidip^{2-}$. The four acetate anions are coordinated to three cobalt ions in two different binding modes. Two of them are linked between Co1 and Co2 ions in $\mu_{1,3}$-acetato mode, the other are bonded to Co1 as monodentate ligand. The distorted octahedral coordination sphere of the central cobalt (Co2) involves an O_6 donor set including four O_{alkoxo} ($pmidip^{2-}$) and two O (acetato) donors. The octahedral coordination sphere of the external cobalt (Co1) shows an N_2O_4 donor set including one N_{py} ($pmidip^{2-}$), N_{amine} ($pmidip^{2-}$), two O_{alkoxo} ($pmidip^{2-}$), and two O (acatato) donors. Two bridging Co1−O1−Co2 and Co1−O2−Co2 angles are

View Article Online
DOI: 10.1039/C6DT02701F

98.21(6) and 95.47(6)°, respectively. The Co^{II}•••Co^{III} distance within the trimeric unit is 3.0045(6) Å, which is shorter than that of **2** (Co^{II}•••Co^{II} 3.1314(2) Å).[21a] The Co^{III}•••Co^{III} (-x, -y+1, -z+1) distance is 6.0090(11) Å and the shortest Co•••Co distance between the trimers is 7.6033(11) Å. The bond angles relating to the external cobalt (Co1) and internal cobalt (Co2) lie from 85.25(8) to 177.00(7)° and 75.02(5) to 180.00(3)°, respectively. Due to the bond angles, the central cobalt (Co2) is closer to octahedral geometry than the external cobalt (Co1). In order to determine the oxidation states of cobalt ions in **3** using the bond lengths of Co−N/O, we have used the bond valence sum (BVS) method. Bond valences (*s*) are obtained using the equation, $s = \exp[(r_o - r)/B]$, where B = 0.37 Å and r_o is used from published tables.[22] The BVS for cobalt ion is then the sum of bond valences for each bond made to the cobalt ion. The BVS calculations give the valence sums of 3.46 for Co1 and 2.12 for Co2. The results indicate that the Co1 and Co2 ions are trivalent and divalent, respectively. That is, this strongly demonstrates the +2 oxidation state for central cobalt ion (Co2) and the +3 oxidation states for terminal cobalt ions (Co1), i.e., Co^{III}(S = 0, LS)−Co^{II}(S = 3/2, HS)−Co^{III}(S = 0, LS).[22]

Magnetic properties. The magnetic susceptibilities, $\chi(T)$, of **1**−**3** were measured between 2 to 300 K (external field 5000~10000 Oe), and plotted as $\mu_{eff}(T)$, Fig. 4. For **1**, at 300 K, the effective magnetic moment, μ_{eff} [= $(8\chi_M T)^{1/2}$], is 5.53 μ_B/Ni_3, and it is nearly constant with decreasing temperature until 50 K. The value of μ_{eff} at room temperature is larger than the 4.90 μ_B expected for independent three S = 1, Ni(II) spins, and is attributed to a high effective g value, i.e. g_{eff} = 2.24. Below 50 K, $\mu_{eff}(T)$ increases abruptly to 6.74 μ_B, at 5 K (Fig. 4). It should be noted that the continuous increase in $\mu_{eff}(T)$ with decreasing temperature from 300 to 5 K is suggestive of ferromagnetic interaction in **1**. The $\chi(T)$ was simulated with the julX program package for exchange coupled systems.[23] The simulation is based on the spin-Hamiltonian operator for a trinuclear system of three high-spin nickel(II) ions with spin $S_a = S_b = S_c = 1$ ($H = -2J(S_a \bullet S_b + S_b \bullet S_c)$).[24] The best fit had J (= J_{ab} = J_{bc}) = +2.35 cm^{-1} and g (= g_a = g_b = g_c) = 2.24. Complex **1** has three exchange pathways, i.e., μ_2-ethoxo, μ_2-acetato, and syn-syn carboxylato. μ_2-Ethoxo and μ_2-acetato bridges can transmit either ferro- or antiferromagnetic interaction depending on Ni-O(ethoxo/acetato)-Ni bridging angles. Furthermore, it is known that the syn-syn conformations of carboxylate ligands cause antiferromagnetic interactions.[25] In **1**, Ni1−O6−Ni2 angle is 91.90(4)° indicating a ferromagnetic interaction via the O6 atom whereas Ni1−O1−Ni2 angle is 100.17(4)° meaning an antiferromagnetic

View Article Online
DOI: 10.1039/C6DT02701F

coupling through the O1 atom. Overall, complex **1** shows a weak ferromagnetic coupling (J = +2.35 cm^{-1}). This can be expected that the pathway of Ni1−O6−Ni2 is the most favorable in the magnetic couplings between the Ni(II) ions. Ghosh et al. have reported two nickel(II) trinuclear complexes $[Ni_3(L)_2(OAc)_4]$ and $[Ni_3(L)_2(OAc)_4(H_2O)_2]$ (HL = 2-[(3-methylamino-propylimino)-methyl]-phenol).[26] In the former, the Ni−O(phenoxido)-Ni bridging angle is 97.63(11)° and the Ni−O(acetato)-Ni bridging angle is 91.87(10)°. Due to the Ni−O(acetato)-Ni angle which is in the range of ferromagnetic couplings, the trinuclear complex shows a very weak ferromagnetic interaction (J = +0.11 cm^{-1}). In the latter, the Ni−O(phenoxido)−Ni bridging angle is 99.89(9)° and the Ni−O(acetato)−Ni bridging angle is 96.49(9)°. Both bridging angles are greater than 93.5° (magic angle).[27] As result, the nickel(II) trimer displays a weak antiferromagnetic coupling (J = −4.3 cm^{-1}).

For **2**, at 265 K, the effective magnetic moment is 7.91 μ_B/Co_3, which is larger than the value of 6.71 μ_B/Co_3 expected for independent three high-spin cobalt(II) ions (g = 2, S = 3/2) because of the strong spin–orbit coupling of cobalt(II) ions. This value decreases gradually with decreasing temperature to 6.72 μ_B/Co_3 at 2 K. The $\mu_{eff}(T)$ data were fit to an analytical expression for a coupled S = 3/2 trinuclear spin model based on the Hamiltonian $H = -2J(S_a \bullet S_b + S_b \bullet S_c)$ ($S_a = S_b = S_c = 3/2$).[23,24] The exact expression of the Hamiltonian includes various factors, i.e. spin-orbit couplig, axial and rhombic distortions, and Zeeman interactions, and we simply used the above Hamiltonian for fitting.[18b,28] The best fit had $J_{ab} = J_{bc} = -0.5$ cm^{-1}, g = 2.37, and θ = −0.4 K. The coupling constants (J_{ab} and J_{bc}) through the bridging oxygen atoms (ethoxo and acetate anions) are expected to be very weak antiferromagnetic. In **2**, the bridging angles of Co1-O6-Co2 (89.56(14)°) and Co1-O1-Co2 (102.92(17)°) are very close to those of Ni1-O6-Ni2 (91.90(4)°) and Ni1-O1-Ni2 (100.17(4)°) of **1**. Interestingly, contrary to **1**, the magnetic properties of **2** indicates an antiferromagnetic coupling between the cobalt(II) ions within the trinuclear unit. This can be expected that the antiferromagnetic coupling is related to the electronic configuration of cobalt(II) ion, i.e., $t_{2g}^5 e_g^2$. That is, the t_{2g} orbital occupied with 5 electrons can be contributed to the magnetic interactions. Likewise, such magnetic interaction is observed in $[Co_3(\mu\text{-}OOCCF_3)_4(\mu\text{-}H_2O)_2(OOCCF_3)_2(H_2O)_2(C_4H_8O_2)]$ (J = −0.4 cm^{-1}).[18b] Consequently, the magnetic properties of **2** indicate that the bridges of ethoxo and acetate anions are rather poor exchange pathways within the trinuclear unit.

Complex **3** consists of two low-spin Co^{III} as wingtip ions and one high-spin Co^{II} as the central ion, i.e., Co^{III}(LS, S = 0)–Co^{II}(HS, S = 3/2)–Co^{III}(LS, S = 0). The wingtip cobalt(III) ions are diamagnetic (S

View Article Online
DOI: 10.1039/C6DT02701F

= 0), whereas the central cobalt(II) ion is paramagnetic (S = 3/2). At room temperature, the effective moment is 4.92 μ_B, suggesting that the cobalt(II) ion is a high-spin state. This value is larger than the spin-only value (3.87 μ_B) for a high-spin Co^{II}, indicative of the strong spin-orbit coupling.[29] On lowering the temperature, $\mu_{eff}(T)$ decreases gradually with decreasing temperature to 3.62 μ_B at 2 K (Fig. 4). The decrease of the effective magnetic moment at low-temperature (<100 K) was most likely due to the strong spin–orbit coupling of Co^{II} ion. Thus the spin-orbit coupling highly contributes to the zero-field splitting (ZFS). $\chi(T)$ for **3** was simulated with the julX program package (ver. 1.4.1).[23] The simulations are based on the usual spin-Hamilton operator for the cobalt trimer (S = 0, S = 3/2, S = 0):

$$H = g\beta \boldsymbol{S}\cdot\boldsymbol{B} + D[S_z^2 - S(S+1)/3 + (E/D)(S_x^2 - S_y^2)] \quad (1)$$

where S is the total spin multiplet (3/2), g is the average electronic g value, D is the axial zero-field splitting parameter, and E/D is the rhombicity of the zero-field splitting. The best fit from the data had g = 2.530, $|D|$ = 36.0 cm^{-1}, and the spin impurity, ρ = 0.005 (TIP = 100×10^{-6} emu/mol).[23] The zero-field splitting parameter between the ±1/2 and ±3/2 Kramers doublets was comparable to those for [Co(DABPH)Br(H_2O)]Br ($|D|$ = 30.0 cm^{-1}), [Co(DABPH)(H_2O)(NO_3)](NO_3) ($|D|$ = 32.0 cm^{-1}) (DABPH = 2,6-diacetylpyridinebis(benzoic acid hydrazone)],[30] and [(Me_3tacn)$_2Co_2(\mu$-Cl)$_3$]BPh_4 ($|D|$ = 40.0 cm^{-1}) (Me_3tacn = 1,4,7-trimethyl-1,4,7-triazacyclononane).[31] Additionally, above 2 K, $\chi_M^{-1}(T)$ can be fit to the Curie-Weiss expression $\chi_M = C/(T-\theta)$ with θ = −7.04 K (C = 3.073 emu K mol^{-1}) for **3**.[32] This value can be also related to large D value and/or intermolecular interactions.

Catalytic properties

Hydrocarbon oxidation catalyzed by cobalt complexes 2 and 3. We examined the catalytic epoxidation of cyclohexene with *m*-chloroperbenzoic acid (MCPBA) as an oxidant in the presence of the complex **2** or **3** as catalyst in various solvent systems. We expected that **2** and **3** with tri-nuclear sites might show better catalytic activities than mono-nuclear ones previously reported, because tri-nuclear systems have three times more pre-catalytic sites than mono-nuclear ones.[33] In protic solvents such as methanol and water, small amounts (less than 20%) of products were produced, while higher yields (50-60%) of epoxides were afforded in aprotic solvents such as CH_3CN and

View Article Online
DOI: 10.1039/C6DT02701F

CH_2Cl_2. In particular, the best yield of epoxide was observed in a mixture of CH_3CN/CH_2Cl_2 (1:1 v/v). In addition, peroxides such as hydrogen peroxide and *tert*-butyl hydroperoxide (*t*-BuOOH) were also tested as a potent oxidant, but they did afford trace amounts of epoxide, indicating that they were incompetent oxidants. As the optimized condition, therefore, MCPBA (0.07 mmol) was added to a mixture of olefin (0.035 mmol) and pre-catalyst (**2** or **3**, 1.24 x 10^{-3} mmol) in CH_3CN/CH_2Cl_2 (1:1 v/v; 1 mL) at room temperature.[33] The epoxidation reaction was complete less than 1 min, and we confirmed that direct substrate oxidation by MCPBA was negligible with time control experiments. Moreover, complexes **2** and **3** seemed to be stable enough during the catalytic reactions according to UV/Vis spectroscopy and XRPD patterns (Figs. S1 and S2).

The epoxidation results obtained under the optimized conditions are summarized in Table 2. With pre-catalyst **2**, cyclic olefins such as cyclopentene, cycloheptene, and cyclooctene were oxidized to the corresponding epoxides (60.8−79.1%; entries 1−3), with conversions in the range of 77.2 to 86.4%. In the case of cyclohexene (entry 4), it afforded the major product cyclohexene oxide (63.9%) along with small amounts of 2-cyclohexene-1-ol (2.8%) and 2-cyclohexene-1-one (2.0%). These results suggest that the radical oxidation reactions were little involved in the epoxidation reaction.[11,34] Terminal olefins such as 1-hexene and 1-octene (entries 5 and 6), well-known as difficult-to-oxidize substrates,[35] were converted to the corresponding epoxides with moderate yields (69.3% and 36.4%; respectively). *cis*-2-Hexene and *cis*-2-octene were used to probe the epoxidation stereochemistry, which were oxidized to *cis*-2-hexene oxide and *cis*-2-octene oxide (28.1% and 30.2%) in addition to *trans*-2-hexene oxide and *trans*-2-octene oxide (32.9% and 30.3%; entries 7 and 9). These results demonstrate that the stereochemical retention were low in this epoxidation reaction. *trans*-2-Hexene and *trans*-2-octene were oxidized to *trans*-2-hexene oxide and *trans*-2-octene oxide (66.8% and 58.5%; entries 8 and 10). Styrene was oxidized to styrene epoxide (22.9%; entry 11), phenylacetaldehyde (58.2%) and benzaldehyde (6.5%). While *cis*-stilbene produced dominantly *trans*-stilbene oxide (54.0%) with some benzaldehyde (20.0%) and *cis*-stilbene oxide (5.7%; entry 12), *trans*-stilbene was converted to *trans*-stilbene oxide (45.3%; entry 13) and benzaldehyde (20.3%). Pre-catalyst **3** was slightly less efficient toward olefin epoxidation reaction than pre-catalyst **2** (columns 5 vs 7 in Table 2). These results indicate that the pre-catalysts **2** and **3** are more selective and efficient than those previously reported for the olefin epoxidation and hydrocarbon hydroxylation.[36] In the previous catalytic systems with di- and tri-nuclear Co complexes, *t*-BuOOH was

View Article Online
DOI: 10.1039/C6DT02701F

often used as an oxidant. It decomposed to *t*-BuO• or *t*-BuOO• species via the homolytic O-O bond cleavage or radical process, which oxidize the olefins or hydrocarbons non-selectively to the products.

Terminal olefins are particularly considered as difficult-to-oxidize olefins because of their electron-deficient nature,[35] while their corresponding products 1,2-epoxides are known as the versatile starting materials for the synthesis of more complicated compounds. Since reasonable yield of terminal epoxide from 1-hexene was obtained with **2** (entry 5 in Table 2), thus, we investigated the terminal olefin epoxidation by using **2**. The results are summarized in Table 3. All of the terminal olefins were oxidized to the corresponding epoxides in moderate yields (34.3−75.0%), with conversions in the range of 47.4−100%, indicating that our catalytic system could be useful for the epoxidation reaction of a variety of terminal olefins.

Product distribution of the O−O bond cleavage of PPAA with complexes 2 or 3. To gain a clearer insight into the reactive oxidants that are involved in olefin epoxidation, we used peroxyphenlyacetic acid (PPAA) as a mechanistic probe, because the cleavage mode could be easily determined by quantitative analysis of the degradation products derived from PPAA.[37] When the O-O bond of the coordinated anion of PPAA undergoes heterolytic O-O bond cleavage or directly oxidizes the substrate, phenylacetic acid (PAA) is produced. On the other hand, the homolytic cleavage of the O-O bond generates an acyloxyl radical, which degrades to benzyl alcohol, benzaldehyde, and toluene.[37a,b] First, a control experiment with PPAA as oxidant under the same reaction conditions as used for MCPBA-epoxidation with pre-catalyst **2** was carried out in the absence of substrate (entry 1 in Table 4). The heterolytic cleavage product, PAA (72.4% based on PPAA), and the homolytic cleavage products, benzaldehyde (14.8%) and benzyl alcohol (3.8%), were formed in a ratio of 79.6:20.4 (column 8). These results suggest that the $Co^{II}Co^{II}Co^{II}$-OOC(O)R species (**4**) formed from the reaction of **2** and MCPBA underwent the partition of simultaneously heterolytic (79.6%) and homolytic (20.4%) O-O bond cleavage to produce $Co^{II}Co^{II}Co^{IV}$=O (**5**) and $Co^{II}Co^{II}Co^{IV}$=O (**6**) species (Scheme 1). Next, we varied the concentration of the substrate to examine the concentration dependence on the ratio of the heterolysis to homolysis. If the $Co^{II}Co^{II}Co^{II}$-OOC(O)R species contributed to the epoxidation reaction, the ratio of heterolysis to homolysis would vary according to the concentration of substrate,[38] because direct olefin epoxidation by $Co^{II}Co^{II}Co^{II}$-OOC(O)R species generates the heterolytic cleavage product, PAA. When we changed the concentration of an easy-to-oxidize substrate, cyclohexene, from 0 to 160 mM, the ratio of the heterolysis increased slightly from

View Article Online
DOI: 10.1039/C6DT02701F

79.6 to 83.8 within possible experimental error, as shown in Table 4 (entries 1-5). These results imply that the $Co^{II}Co^{II}Co^{II}$-OOC(O)R species are a little involved in this oxidation reaction when the concentration of cyclohexene is very high. We changed the substrate from cyclohexene to a difficult-to-oxidize olefin, 1-octene, to examine the cleavage mode of PPAA on the type of substrate.[38a] The partition of the heterolysis and the homolysis was nearly identical, without respective to 1-octene concentration (entries 1-5 in Table 5), suggesting that the $Co^{II}Co^{II}Co^{II}$-OOC(O)R species would not be involved in the epoxidation of 1-octene, even in the presence of the high concentration of it. Analogous results were also obtained for **3** (entries 6-10 in Tables 4 and 5).

Based on the product distributions of the O−O bond cleavage of PPAA, we propose the plausible olefin epoxidation mechanism catalyzed by the pre-catalyst **2** with peracids (Scheme 1). **2** reacts with peracid to form $Co^{II}Co^{II}Co^{II}$-OOCCO)R intermediate (**4**), which underwent the O-O bond cleavage to ~75% heterolysis (pathway (a)) and ~25% homolysis (pathway (c)) to produce $Co^{II}Co^{II}Co^{IV}$=O (**5**) and $Co^{II}Co^{II}Co^{III}$=O (**6**) species, respectively. We assume that the active oxidant $Co^{II}Co^{II}Co^{IV}$=O (**5**) might be responsible for efficient olefin epoxidation and the radical types of the products stem from the intermediate $Co^{II}Co^{II}Co^{III}$=O (**6**). Moreover, the intermediate Co^{III}-OOC(O)R species could contribute a little to the catalytic epoxidation in the presence of the easy-to-oxidize olefin (pathway (b)), while it was inactive with the difficult-to-oxidize substrate such as 1-octene. Similar olefin-epoxidation mechanism can be proposed for the pre-catalyst **3** (Scheme S1).

On the other hand, the difference of the catalytic activities between **2** and **3** may be explained with the presence of the proton of the ethanol moiety in the complex **2**, which might act as a general acid catalyst for promoting the heterolytic O-O bond cleavage of Co-acylperoxide intermediate **4**.

Conclusions

We have prepared and characterized three novel trinuclear compounds using H_2pmide/H_2pmidip and Ni(II)/Co(II) metal ions. **1** is a trinuclear nickel(II) complex showing ferromagnetic coupling between nickel(II) ions within trimeric unit, whereas **2** is a trinuclear cobalt(II) complex showing weak antiferromagnetic coupling between cobalt(II) ions within the trimer. **1** and **2** have isomorphous structures. **3** has different bonding modes, although the trinuclear cobalt complex of **3** is bridged by ethoxo and acetato ligands. Different to **2**, **3** is a mixed-valence trinuclear cobalt complex, Co^{III}(S = 0)–Co^{II}(S = 3/2)–Co^{III}(S =0) and displays the magnetic properties (large D value) of a cobalt(II) ion in a

View Article Online
DOI: 10.1039/C6DT02701F

high-spin state. Complexes **2** and **3** showed significant catalytic activities toward various olefins with modest to good yields. Complex **3** was slightly less efficient toward olefin epoxidation reaction than complex **2**. Also complex **2** was used for terminal olefin oxidation reaction and showed the oxidation to the corresponding epoxides in moderate yields with conversions. The cobalt pre-catalysts **2** and **3** promoted the O-O bond cleavage to ~75% heterolysis and ~25% homolysis. The intermediate Co-OOC(O)R species might contribute a little to the catalytic epoxidation in the presence of the easy-to-oxidize olefin.

Acknowledgements

This research was supported by Basic Science Research Program through the National Research Foundation of Korea (NRF) funded by the Ministry of Education, Science and Technology (No. 2015R1D1A1A01059872 and 2014R1A2A1A11051794). We thank Prof. Joel S. Miller and J. E. Sussman for obtaining the magnetic data of **2**. X-ray crystallography at the PLS-II 2D-SMC beamline was supported in part by MEST and POSTECH.

View Article Online
DOI: 10.1039/C6DT02701F

Table 1 Summary of the crystallographic data for **1**−**3**

Compound	**1**	**2**	**3**
Empirical formula	$C_{28}H_{42}N_4Ni_3O_{12}$	$C_{28}H_{42}Co_3N_4O_{12}$	$C_{32}H_{48}Co_3N_4O_{12}$
Formula weight	802.73	803.45	857.53
Crystal system	Monoclinic	Monoclinic	Monoclinic
Space group	$P2_1/n$	$P2_1/n$	$P2_1/c$
a (Å)	11.479(2)	11.6737(12)	7.9190(16)
b (Å)	10.789(2)	10.8739(12)	23.274(5)
c (Å)	13.770(3)	13.8627(15)	9.4900(19)
α (°)	90	90	90
β (°)	113.00(3)	112.781(2)	94.12(3)
γ (°)	90	90	90
V (Å^3)	1569.8(6)	1622.4(3)	1744.5(6)
Z	2	2	2
d_{calc} (g cm^{-3})	1.698	1.645	1.632
λ (Å)	0.63000	0.71073	0.63000
T (K)	102(2)	200(2)	100(2)
μ (mm^{-1})	1.329	1.584	1.060
F(000)	836	830	890
Reflections collected	22005	11458	21064
Independent reflections	6179	4020	5861
Reflections with $I>2\sigma(I)$	5971	2699	4241
Goodness-of-fit on F^2	1.037	1.149	1.027
R_1[a] [$I>2\sigma(I)$]	0.0281	0.0534	0.0445
wR_2[b] [$I>2\sigma(I)$]	0.0776	0.1221	0.1155
CCDC no.	1456726	1456727	1456728

[a] $R_1 = \Sigma||F_o| - |F_c||/\Sigma|F_o|$. [b] $wR_2 = [\Sigma w(F_o^2 - F_c^2)^2/\Sigma w(F_o^2)^2]^{1/2}$.

View Article Online
DOI: 10.1039/C6DT02701F

Table 2 Olefin epoxidations by MCPBA with cobalt complexes **2** and **3** in CH_2Cl_2/CH_3CN (1:1) at room temperature[a]

Entry	Substrate	Product	**2**		**3**	
			Conversion [%][b]	Yield [%][b]	Conversion [%][b]	Yield [%][b]
1	cyclopentene	epoxide	80.3±0.5	68.8±0.7	76.3±0.2	49.2±5.7
2	cycloheptene	epoxide	86.4±2.5	79.1±0.9	80.9±0.8	77.9±0.6
3	cyclooctene	epoxide	77.2±3.6	60.8±0.4	75.2±0.7	59.2±1.5
4	cyclohexene	epoxide	70.0±0.8	63.9±4.8	73.7±1.0	55.2±2.6
		2-cyclohexene-1-ol		2.8±0.9		2.1±0.1
		2-cyclohexene-1-one		2.0±0.4		4.1±0.1
5	1-hexene	epoxide	75.8±8.0	69.3±0.1	55.1±0	29.4±1.1
6	1-octene	epoxide	70.8±2.4	36.4±0.4	57.2±0.3	33.0±0.2
7	*cis*-2-hexene	*cis*-oxide	82.4±1.0	28.1±0.5	70.8±5.0	29.7±3.7
		trans-oxide		32.9±0.2		36.5±4.4
8	*trans*-2-hexene	*trans*-oxide	89.9±3.6	66.8±1.3	72.3±7.1	54.5±4.9
9	*cis*-2-octene	*cis*-oxide	82.6±0.6	30.2±0.4	79.8±0.4	27.1±0.8
		trans-oxide		30.3±0		32.1±0.6
10	*trans*-2-octene	*trans*-oxide	80.3±4.4	58.5±0.7	82.6±0.7	50.0±0.8
11	styrene	epoxide	97.5±2.5	22.9±1.4	92.5±2.0	37.7±1.3
		benzaldehyde		6.5±1.0		6.2±0.1
		phenylacetaldehyde		58.2±0.2		3.5±0.1
12	*cis*-stilbene	*cis*-stilbene oxide	84.4±1.5	5.7±0.7	88.0±0.1	7.0±0.2
		trans-stilbene oxide		54.0±2.3		33.5±2.8
		benzaldehyde		20.0±0.9		15.4±0.6
		2-phenylacetophenone				5.7±0.4
13	*trans*-stilbene	*trans*-stilbene oxide	94.7±0.8	45.3±0.4	96.6±0.4	47.0±5.0
		benzaldehyde		20.3±2.9		16.3±0.1
		2-phenylacetophenone				5.8±0.1

[a] Reaction conditions: olefins (0.035 mmol), complexes (1.24×10^{-3} mmol), MCPBA (0.07 mmol), and solvent (1 mL, CH_2Cl_2/CH_3CN =1:1). [b] Based on substrate.

View Article Online
DOI: 10.1039/C6DT02701F

Table 3 Terminal olefin epoxidations by MCPBA with cobalt complex **2** in CH_2Cl_2/CH_3CN (1:1) at room temperature[a]

Entry	Substrate	Product	Conversion (%)[b]	Yield (%)[b]
1	1-hexene	1,2-epoxyhexane	100±0	70.1±0.5
2	1-octene	1,2-epoxyoctane	98.2±0.6	54.5±0.3
3	1-nonene	1,2-epoxynonane	52.0±1.0	45.6±0.3
4	1-decene	1,2-epoxydecane	98.4±0.1	50.6±1.9
5	1-undecene	1,2-epoxyundecane	95.2±0.9	48.9±1.2
6	1-dodecene	1,2-epoxydodecane	96.8±0.4	53.1±0.5
7	1-tridecene	1,2-epoxytridecane	97.4±0.6	48.5±0.4
8	1-tetradecene	1,2-epoxytetradecane	95.9±1.5	34.3±2.6
9	1-pentadecene	1,2-epoxypentadecane	96.2±0.5	46.1±0.6
10	1-hexadecene	1,2-epoxypentadecane	95.8±1.0	75.0±3.2
11	1-octadecene	1,2-epoxypentadecane	91.2±1.5	61.2±1.9
12	vinylcyclohexane	2-cyclohexyloxirane	47.4±0.4	46.2±1.0

[a] Reaction conditions: olefin (0.035 mmol), complex (1.24×10^{-3} mmol), MCPBA (0.13 mmol), and solvent (1 mL, CH_2Cl_2/CH_3CN =1:1). [b] Based on substrate.

Table 4 Yield of products derived from PPAA mediated by the cobalt complexes **2** and **3** in the absence and the presence of cyclohexene in a mixture of CH_3CN/CH_2Cl_2 (1:1) at room temperature[a]

Entry	Complex	Cyclohexene [mM]	Heterolysis[b]	Homolysis[b]			Hetero (**5**)/ Homo (**6**+**7**+**8**)	Oxidation products		
			PAA **(5)**	Benzaldehyde **(6)**	Benzyl alcohol **(7)**	Toluene **(8)**		oxide[c]	-ol[c]	-one[c]
1	**2**	0	72.4±0.3	14.8±0	3.8±0.4	-	**3.89** (79.6/20.4)	-	-	-
2	**2**	20	75.9±0.3	16.6±0.9	4.8±0.1	-	**3.55** (78.0/22.0)	34.5±0.2[d]	0[d]	3.8±0.1[d]
3	**2**	40	78.7±0.6	15.7±0.2	4.2±0.1	-	**3.95** (79.8/20.2)	22.6±0.6[d]	0[d]	3.2±0.2[d]
4	**2**	80	72.4±5.2	12.6±0.9	4.0±0.2	-	**4.36** (81.3/18.7)	24.8±2.4[e]	0[e]	3.8±1.0[e]
5	**2**	160	78.1±4.3	11.4±0.2	3.7±0.1	-	**5.17** (83.8/16.2)	26.4±0.5[e]	0.9±0.1[e]	3.7±0.1[e]
6	**3**	0	59.5±2.5	14.3±0	4.5±0.1	-	**3.16** (76.0/24.0)	-	-	-
7	**3**	20	59.7±5.0	16.7±0.1	4.5±0	-	**2.82** (73.8/26.2)	24.8±0.1[d]	5.8±0.2[d]	3.4±0.1[d]
8	**3**	40	65.9±0.9	16.0±0.2	4.4±0.1	-	**3.23** (76.4/23.6)	16.7±1.0[d]	4.1±0.3[d]	2.5±0.2[d]
9	**3**	80	68.2±2.3	15.6±0.1	4.3±0.3	-	**3.43** (77.4/22.6)	21.7±1.2[e]	6.8±0[e]	4.2±0[e]
10	**3**	160	71.8±1.6	14.1±0.1	4.2±0	-	**3.92** (79.7/20.3)	30.5±2.4[e]	12.2±0.3[e]	8.5±0.1[e]

[a] Reaction conditions: substrate (0-0.16 mmol), complex (1.24×10^{-3} mmol), PPAA (0.04 mmol), and solvent (1 mL, CH_3CN/CH_2Cl_2=1:1). [b] Based on PPAA; **5-8** indicate phenylacetic acid, benzaldehyde, benzyl alcohol, and toluene, respectively. [c] -ol, -one, and oxide indicate 2-cyclohexen-1-ol, 2-cyclohexen-1-one, and cyclohexene oxide, respectively. [d] Based on substrate, cyclohexene. [e] Based on oxidant, PPAA.

Table 5 Yield of products derived from PPAA mediated by the cobalt complexes **2** and **3** in the absence and the presence of 1-octene in a mixture of CH_3CN/CH_2Cl_2 (1:1) at room temperature[a]

Entry	Complex	Cyclohexene [mM]	Heterolysis[b]	Homolysis[b]			Hetero (**5**)/ Homo (**6**+**7**+**8**)	Oxidation products
			PAA (5)	Benzaldehyde **(6)**	Benzyl alcohol **(7)**	Toluene **(8)**		1-octene oxide
1	**2**	0	72.4±0.3	14.8±0	3.8±0.4	-	**3.89** (79.6/20.4)	-
2	**2**	20	70.1±2.8	16.7±0.2	4.3±0.1	-	**3.34** (77.0/33.0)	18.0±0.6[c]
3	**2**	40	68.9±0.7	18.2±0.4	4.7±0.1	-	**3.01** (75.1/24.9)	10.7±1.2[c]
4	**2**	80	67.6±5.6	19.0±1.4	4.6±0.1	-	**2.86** (74.1/25.9)	15.0±0.6[d]
5	**2**	160	68.2±3.9	18.4±0.2	4.4±0	-	**3.04** (75.2/24.8)	16.2±1.2[d]
6	**3**	0	59.5±2.5	14.3±0	4.5±0.1	-	**3.16** (76.0/24.0)	-
7	**3**	20	61.9±6.1	16.1±0.2	4.5±0.2	-	**3.00** (75.0/25.0)	15.0±1.0[c]
8	**3**	40	62.7±1.4	16.8±0.1	4.4±0.1	-	**2.96** (74.7/25.3)	9.6±0.2[c]
9	**3**	80	67.9±1.1	17.5±0.1	4.5±0.1	-	**3.09** (75.6/24.4)	11.2±0.1[d]
10	**3**	160	63.8±1.0	17.1±0	4.4±0.1	-	**2.97** (74.8/25.2)	12.9±0.3[d]

[a] Reaction conditions: substrate (0-0.16 mmol), complex (1.24×10^{-3} mmol), PPAA (0.04 mmol), and solvent (1 mL, CH_3CN/CH_2Cl_2=1:1). [b] Based on PPAA; **5-8** indicate phenylacetic acid, benzaldehyde, benzyl alcohol, and toluene, respectively. [c] Based on substrate, 1-octene. [d] Based on oxidant, PPAA.

View Article Online
DOI: 10.1039/C6DT02701F

Figure captions

Fig. 1 Structure of $[(Hpmide)_2Ni_3(CH_3COO)_4]$ (**1**). The atoms are represented by 50% probable thermal ellipsoids. The hydrogen atom on the hydroxyl group is shown as small open circle; all other H-atoms are omitted for clarity.

Fig. 2 Structure of $[(Hpmide)_2Co_3(CH_3COO)_4]$ (**2**). The atoms are represented by 20% probable thermal ellipsoids. The hydrogen atom on the hydroxyl group is shown as small open circle; all other H-atoms are omitted for clarity.

Fig. 3 Structure of $[(pmidip)_2Co_3(CH_3COO)_4]$ (**3**). The atoms are represented by 40% probable thermal ellipsoids. The hydrogen atoms are omitted for clarity.

Fig. 4 Temperature dependence of $\mu_{eff}(T)$ for **1** (○), **2** (×), and **3** (□). Solid lines represent best fits by using parameters given in the text.

Scheme 1 Plausible olefin epoxidation mechanism catalyzed by **2** with peracids.

View Article Online
DOI: 10.1039/C6DT02701F

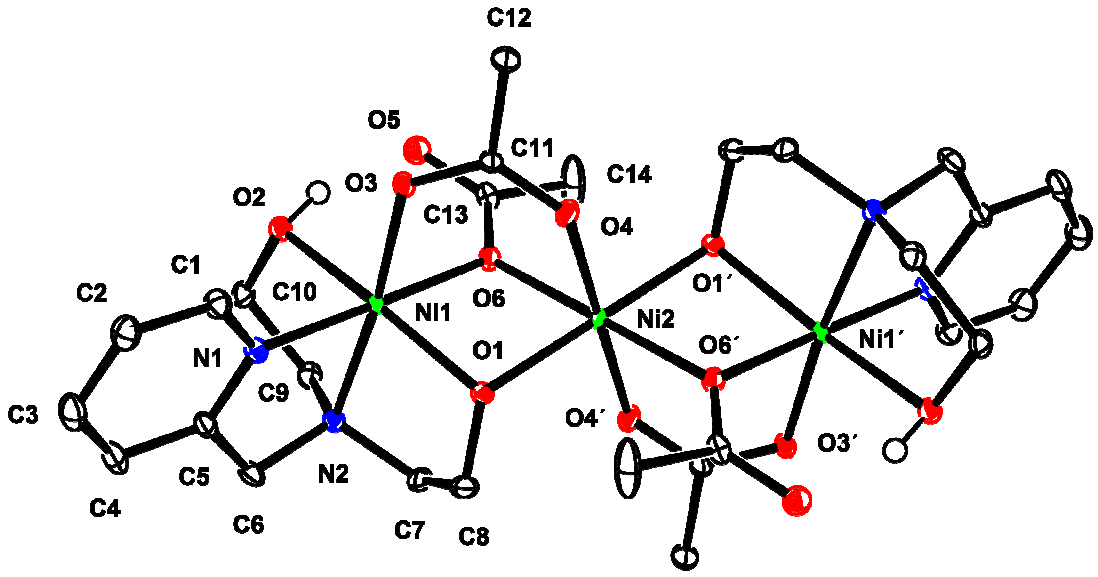

Fig. 1 Structure of $[(Hpmide)_2Ni_3(CH_3COO)_4]$ (**1**). The atoms are represented by 50% probable thermal ellipsoids. The hydrogen atom on the hydroxyl group is shown as small open circle; all other H-atoms are omitted for clarity.

View Article Online
DOI: 10.1039/C6DT02701F

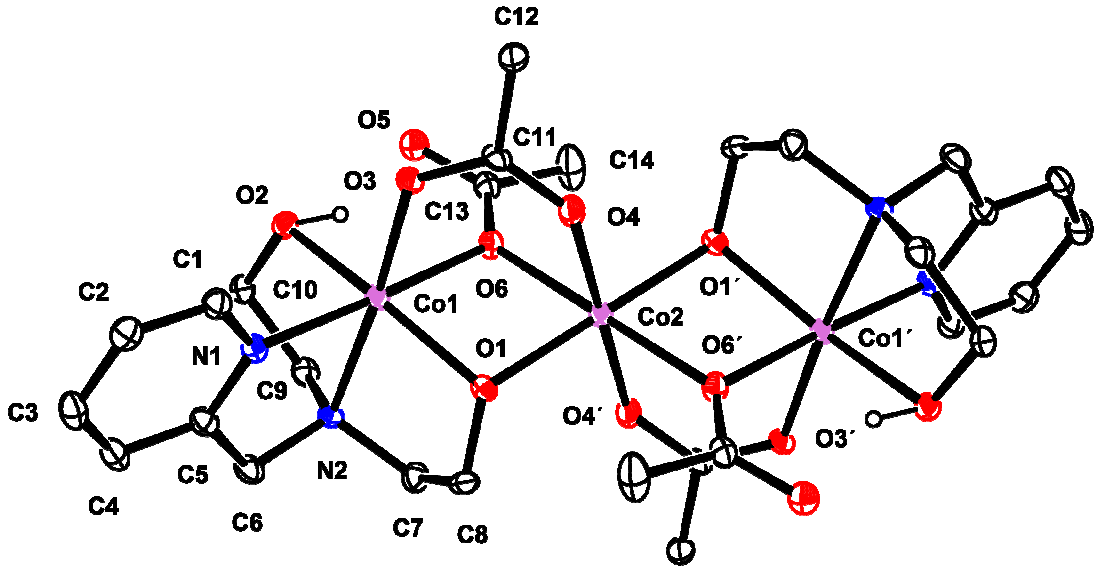

Fig. 2 Structure of $[(Hpmide)_2Co_3(CH_3COO)_4]$ (**2**). The atoms are represented by 20% probable thermal ellipsoids. The hydrogen atom on the hydroxyl group is shown as small open circle; all other H-atoms are omitted for clarity.

View Article Online
DOI: 10.1039/C6DT02701F

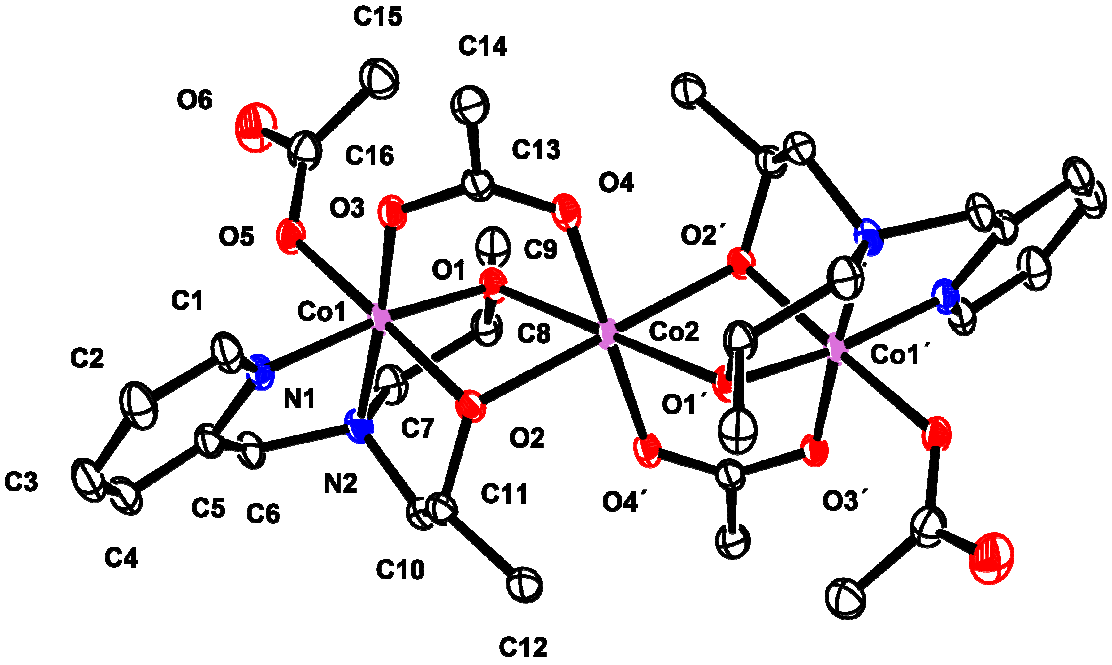

Fig. 3 Structure of $[(pmidip)_2Co_3(CH_3COO)_4]$ (**3**). The atoms are represented by 40% probable thermal ellipsoids. The hydrogen atoms are omitted for clarity.

View Article Online
DOI: 10.1039/C6DT02701F

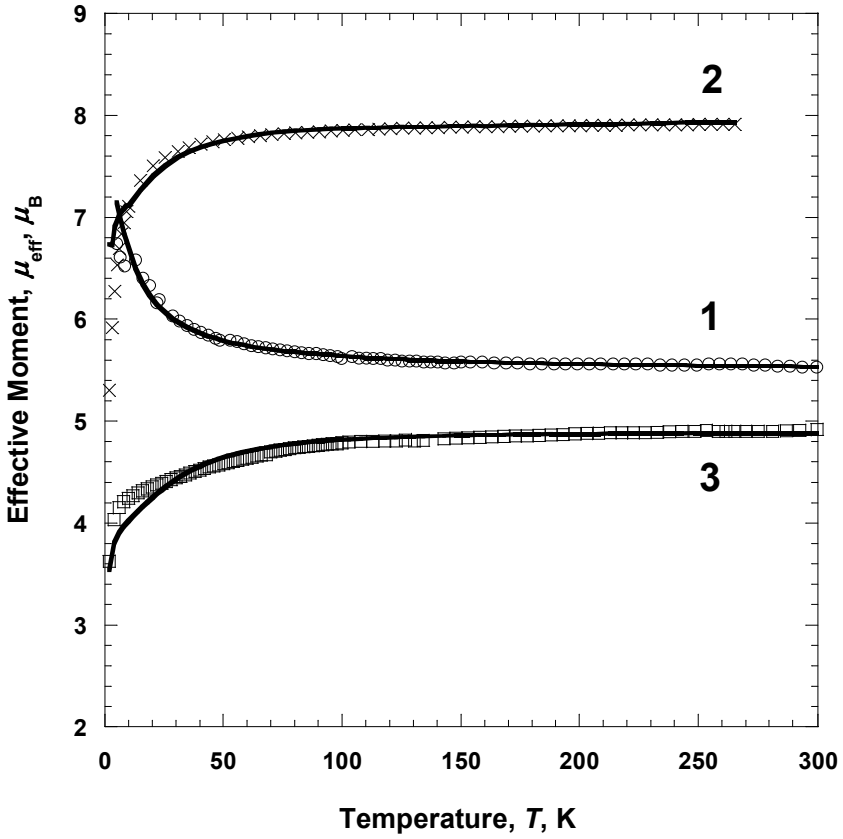

Fig. 4 Temperature dependence of μ_{eff} for **1** (○), **2** (×), and **3** (□). The solids lines are the best-fit curves.

View Article Online
DOI: 10.1039/C6DT02701F

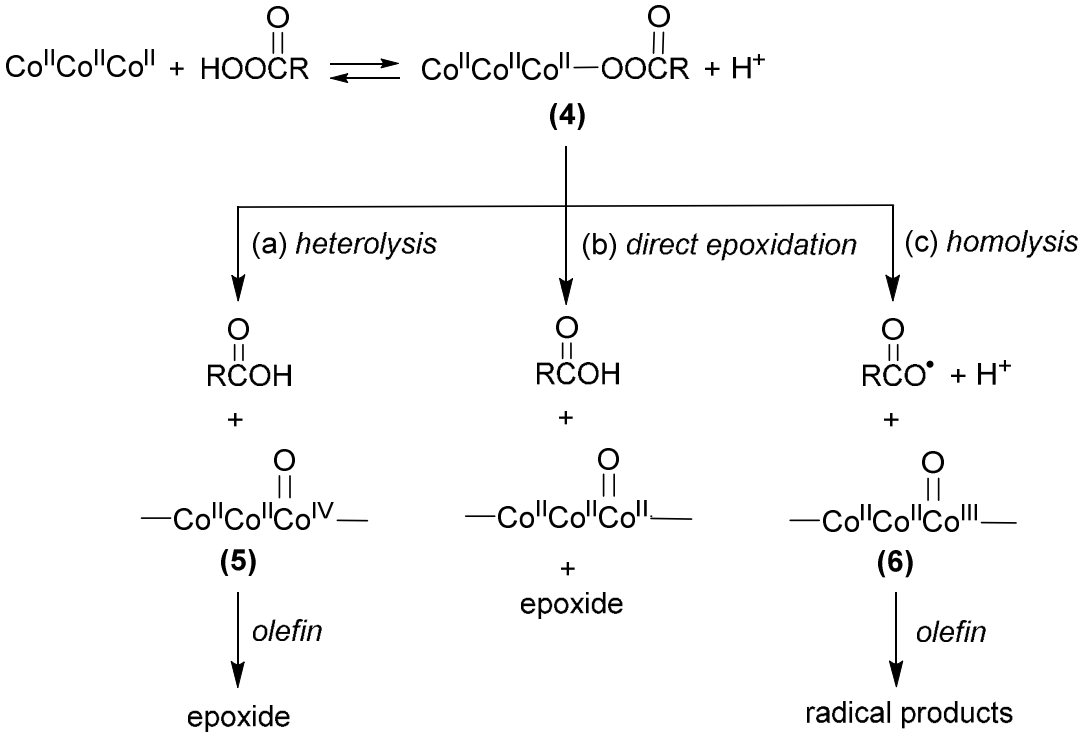

Scheme 1 Plausible olefin epoxidation mechanism catalyzed by **2** with peracids.

View Article Online
DOI: 10.1039/C6DT02701F

References

(1) (a) Y.–Q. Hu, M.–H. Zeng, K. Zhang, S. Hu, F.–F. Zhou and M. Kurmoo, *J. Am. Chem. Soc.*, 2013, **135**, 7901; (b) C. Cañada-Vilalta, W. E. Streib, J. C. Huffman, T. A. O´Brien, E. R. Davidson and G. Christou, *Inorg. Chem.*, 2004, **43**, 101; (c) S. K. Mandal, V. G. Jr. Young and L. Jr. Que, *Inorg. Chem.*, 2000, **39**, 1831; (d) M. Lamouchi, E. Jeanneau, G. Novitchi, D. Luneau, A. Brioude and C. Desroches, *Inorg. Chem.*, 2014, **53**, 63.

(2) (a) B. Sarkar, D. Schweinfurth, N. Deibel and F. Weisser, *Coord. Chem. Rev.*, 2015, **293**–**294**, 250; (b) V. Tudor, G. Marin, F. Lloret, V. C. Kravtsov, Y. A. Simonov, M. Julve and M. Andruh, *Inorg. Chim. Acta*, 2008, **361**, 3446; (c) P. J. Zinn, T. N. Sorrell, D. R. Powell, V. W. Day and A. S. Borovik, *Inorg. Chem.*, 2007, **46**, 10120; (d) H. A. Burkill, N. Robertson, R. Vilar, A. J. P. White and D. J. Williams, *Inorg. Chem.*, 2005, **44**, 3337.

(3) (a) T. M. Powers and T. Betley, *J. Am. Chem. Soc.*, 2013, **135**, 12289; (b) K. Singh, J. R. Long and P. Stavropoulos, *Inorg. Chem.*, 1998, **37**, 1073; (c) M.-L. Louillat and F. W. Patureau, *Org. Lett.*, 2013, **15**, 164; (d) S. Pullen, H. Fei, A. Orthaber, S. M. Cohen and S. Ott, *J. Am. Chem. Soc.*, 2013, **135**, 16997; (e) S. Signorella, A. Rompel, K. Büldt-Karentzopoulos, B. Krebs, V. L. Pecoraro and J.-P. Tuchagues, *Inorg. Chem.*, 2007, **46**, 10864.

(4) (a) B. Biswas, U. Pieper, T. Weyhermüller and P. Chaudhuri, *Inorg. Chem.*, 2009, **48**, 6781; (b) R. Shakya, A. Jozwiuk, D. R. Powell and R. P. Houser, *Inorg. Chem.*, 2009, **48**, 4083; (c) M. Fondo, N. Ocampo, A. M. García-Deibe, E. Ruíz, J. Tercero and J. Sanmartín, *Inorg. Chem.*, 2009, **48**, 9861; (d) B. Li, Z. Li, R.-J. Wei, F. Yu, X. Chen, Y.-P. Xie, T.-L. Zhang and J. Tao, *Inorg. Chem.*, 2015, **54**, 3331; (e) X. Chen, Z. Li, R.-J. Wei, B. Li, T.-L. Zhang and J. Tao, *New J. Chem.,* 2015, **39**, 7333.

(5) (a) J. Manzur, H. Mora, A. Vega, D. Venegas-Yazigi, M. A. Novak, J. R. Sabino, V. Paredes-García and E. Spodine, *Inorg. Chem.*, 2009, **48**, 8845; (b) F. Li, M. Wang, P. Li, T. Zhang and L. Sun, *Inorg. Chem.*, 2007, **46**, 9364; (c) J. W. Shin, A. R. Jeong, K. S. Min, S. Hayami and D. Moon, *Inorg. Chem. Comm.*, 2015, **51**, 46.

(6) (a) J. W. Shin, S. R. Rowthu, B. G. Kim and K. S. Min, *Dalton Trans.*, 2010, **39**, 2765; (b) J. W. Shin,

View Article Online
DOI: 10.1039/C6DT02701F

S. R. Rowthu, M. Y. Hyun, Y. J. Song, C. Kim, B. G. Kim and K. S. Min, *Dalton Trans.*, 2011, **40**, 5762.

(7) J. W. Shin, J. M. Bae, C. Kim and K. S. Min, *Dalton Trans.*, 2014, **43**, 3999.

(8) J. W. Shin, A. R. Jeong, S. Hayami, D. Moon and K. S. Min, *Inorg. Chem. Front.*, 2015, **2**, 763.

(9) R. W. Saalfrank, I. Bernt and F. Hampel, *Chem.– Eur. J.*, 2001, **7**, 2770.

(10) C.–C. Wu, S. Datta, W. Wernsdorfer, G.–H. Lee, S. Hill and E.–C. Yang, *Dalton Trans.*, 2010, **39**, 10160.

(11) S. H. Lee, J. H. Han, H. Kwak, S. J. Lee, E. Y. Lee, H. J. Kim, J. H. Lee, C. Bae, S. N. Lee, Y. Kim and C. Kim, *Chem.–Eur. J.*, 2007, **13**, 9393.

(12) A. J. Arvai and C. Nielsen, *ADSC Quantum-210 ADX Program; Area Detector System Corporation*, Poway, CA, USA, 1983.

(13) Z. Otwinowski and W. Minor, in *Methods in Enzymology*, ed. C. W. Carter Jr. and R. M. Sweet, Academic Press, New York, 1997; Vol. 276, part A, p 307.

(14) *Saint Plus*, Version 6.02, Bruker Analytical X-ray, Madison, WI, 1999.

(15) G. M. Sheldrick, *Acta Crystallogr., Sect. A*, 1990, **46**, 467.

(16) G. M. Sheldrick, *Acta Crystallogr., Sect. A*, 2008, **64**, 112.

(17) K. Nakamoto, *Infrared and Raman Spectra of Inorganic and Coordination Compounds*, 6th ed., John Wiley and Sons, Inc., New Jersey, 2009, Part B, pp 64-70.

(18) (a) L.–L. Hu, Z.–Q. Jia, J. Tao, R.–B. Huang and L.–S. Zheng, *Dalton Trans.*, 2008, 6113; (b) T. Yi, H.-C. Chang, S. Gao and S. Kitagawa, *Eur. J. Inorg. Chem.*, 2006, 1381.

(19) M.–X. Yao, M.–H. Zeng, H.–H. Zou, Y.–L. Zhou and H. Liang, *Dalton Trans.*, 2008, 2428.

(20) K. S. Min, A. G. DiPasquale, A. L. Rheingold, H. S. White and J. S. Miller, *J. Am. Chem. Soc.*, 2009, **131**, 6229.

(21) (a) L. Antolini, A. C. Fabretti, D. Gatteschi, A. Giusti and R. Sessoli, *Inorg. Chem.*, 1991, **30**, 4858; (b) Y.–L. Zhang, S.–P. Chen and S.–L. Gao, *Z. Anorg. Allg. Chem.*, 2009, **635**, 537.

(22) (a) W. Liu and H. H. Thorp, *Inorg. Chem.*, 1993, **32**, 4102; (b) I. D. Brown and D. Altermatt, *Acta Crystallogr. Sect. B Struct. Sci.*, 1985, **41**, 244; (c) N. E. Brese and M. O'Keeffe, *Acta Crystallogr. Sect. B Struct. Sci.*, 1991, **47**, 192; (d) R. M. Wood, K. A. Abboud, R. C. Palenik and G. J. Palenik, *Inorg. Chem.*, 2000, **39**, 2065; (e) J. Zachara, *Inorg. Chem.*, 2007, **46**, 9760.

View Article Online
DOI: 10.1039/C6DT02701F

(23) E. Bill, *julX program, version 1.4.1*, Max Planck Institute for Bioinorganic Chemistry, Mülheim an der Ruhr, Germany, 2008.

(24) O. Kahn, *Molecular Magnetism*, VCH, New York, 1993, pp. 211–249.

(25) (a) K. K. Nanda, R. Das, L. K. Thompson, K. Venkatsubramanian, P. Paul and K. Nag, *Inorg. Chem.*, 1994, **33**, 1188; (b) P. Mukherjee, M. G. B. Drew, C. J. Gomez-García and A. Ghosh, *Inorg. Chem.*, 2009, **48**, 5848.

(26) P. Mukherjee, M. G. B. Drew, C. J. Gómez-García and A. Ghosh, *Inorg. Chem.*, 2009, **48**, 4817.

(27) X.–H. Bu, M. Du, L. Zhang, D.–Z. Liao, J.–K. Tang, R.–H. Zhang and M. Shionoya, *J. Chem. Soc. Dalton Trans.*, 2001, 593.

(28) Z. Tomkowicz, S. Ostrovsky, H. Müller-Bunz, A. J. Hussein Eltmimi, M. Rams, D. A. Brown and W. Haase, *Inorg. Chem.*, 2008, **47**, 6956.

(29) (a) L.–C. Wu, T.–C. Weng, I.–J. Hsu, Y.–H. Liu, G.–H. Lee, J.–F. Lee and Y. Wang, *Inorg. Chem.*, 2013, **52**, 11023; (b) M. Rat, R. A. de Sousa, A. Tomas, Y. Frapart, J. P. Tuchagues and I. Artaud, *Eur. J. Inorg. Chem.*, 2003, 759.

(30) (a) L. J. Batchelor, M. Sangalli, R. Guillot, N. Guihéry, R. Maurice, F. Tuna and T. Mallah, *Inorg. Chem.*, 2011, **50**, 12045; (b) X.–C. Huang, C. Zhou, D. Shao and X.–Y. Wang, *Inorg. Chem.*, 2014, **53**, 12671.

(31) U. Bossek, D. Nühlen, E. Bill, T. Glaser, C. Krebs, T. Weyhermüller, K. Wieghardt, M. Lengen and A. X. Trautwein, *Inorg. Chem.*, 1997, **36**, 2834.

(32) E. Shurdha, C. E. Moore, A. L. Rheingold and J. S. Miller, *Inorg. Chem.*, 2011, **50**, 10546.

(33) The pre-catalytic site or the pre-catalyst means that the complexes 2 and 3 themselves or the destructured complexes 2 and 3 act as catalyst, because the structures of complexes 2 and 3 could be kept or destructured during the catalytic reaction.

(34) (a) T. K. M. Shing, Y. Y. Yeung and P. L. Su, *Org. Lett.*, 2006, **8**, 3149; b) R. A. Sheldon and J. K. Kochi, *Metal-Catalyzed Oxidations of Organic Compounds*, Academic Press, New York, 1981, Chapter 2.

(35) (a) G. Dubois, A. Murphy and T. D. P. Stack, *Org. Lett.*, 2003, **5**, 2469; (b) I. Garcia-Bosch, X. Ribas and M. Costas, *Adv. Synth. Catal.*, 2009, **351**, 348; (c) D. C. Duncan, R. C. Chambers, E. Hecht and

View Article Online
DOI: 10.1039/C6DT02701F

C. L. Hill, *J. Am. Chem. Soc.*, 1995, **117**, 681; (d) J. P. Collman, Z. Wang, A. Straumanis and M. Quelquejeu, *J. Am. Chem. Soc.*, 1999, **121**, 460; (e) H. Tian, X. She, J. Xu and Y. Shi, *Org. Lett.*, 2001, **3**, 1929; (f) M. C. White, A. G. Doyle and E. N. Jacobsen, *J. Am. Chem. Soc.*, 2001, **123**, 7194; (g) X. Zuwei, Z. Ning, S. Yu and L. Kunlan, *Science*, 2001, **292**, 1139.

(36) (a) R. Alam, K. Pal, B. K. Shaw, M. Dolai, N. Pal, S. K. Saha and M. Ali, *Polyhedron*, 2016, **106**, 84; (b) L. Rodionova, A. V. Smirnov, N. E. Borisova, V. N. Khrustalev, A. A. Moiseeva and W. Grunert, *Inorg. Chim. Acta*, 2012, **392**, 221; (c) I. Karthikeyan, S. K. Alamsetti and G. Sekar, *Organometallics*, 2014, **33**, 1665.

(37) (a) S. H. Lee, L. Xu, B. K. Park, Y. V. Mironov, S. H. Kim, Y. J. Song, C. Kim, Y. Kim and S.–J. Kim, *Chem.–Eur. J.*, 2010, **16**, 4678; (b) Y. J. Song, M. Y. Hyun, J. H. Lee, H. G. Lee, J. H. Kim, S. P. Jang, J. Y. Noh, Y. Kim, S. J. Kim, S. J. Lee and C. Kim, *Chem.–Eur. J.*, 2012, **18**, 6094; (c) R. E. White, S. G. Sligar and M. J. Coon, *J. Biol. Chem.*, 1980, **255**, 11108; (d) T. G. Traylor, W. A. Lee and D. V. Stynes, *J. Am. Chem. Soc.*, 1984, **106**, 755; (e) T. G. Traylor, S. Tsuchiya, Y. S. Byun and C. Kim, *J. Am. Chem. Soc.*, 1993, **115**, 2775; (f) Y. J. Song, S. H. Lee, H. M. Park, S. H. Kim, H. G. Goo, G. H. Eoom, J. H. Lee, M. S. Lah, Y. Kim, S.–J. Kim, J. E. Lee, H.–I. Lee and C. Kim, *Chem.–Eur. J.*, 2011, **17**, 7336.

(38) (a) N. Suzuki, T. Higuchi and T. Nagano, *J. Am. Chem. Soc.*, 2002, **124**, 9622; (b) J. T. Groves and Y. Watanabe, *Inorg. Chem.*, 1986, **25**, 4808.

View Article Online
DOI: 10.1039/C6DT02701F

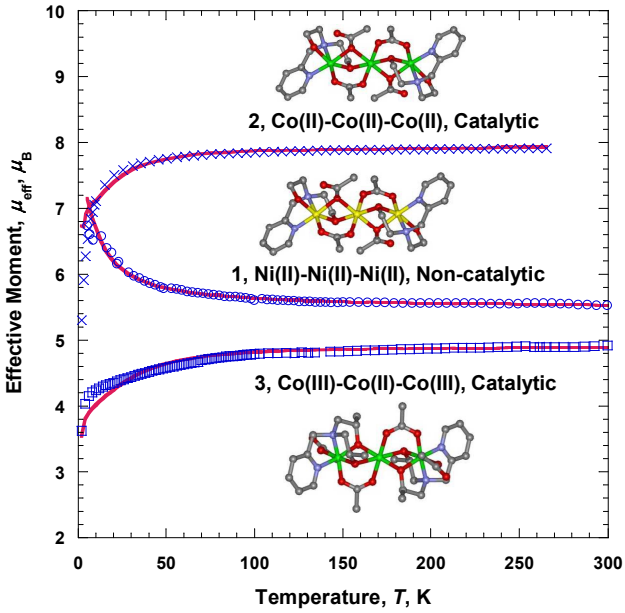

1 shows a ferromagnetic coupling, and **2** and **3** displayed significant catalytic activities toward various olefins with good yields.